OPTOELECTRONİCS AND ADVANCED MATERİALS – RAPID COMMUNICATIONS Vol. 6, No. 1-2, January-February 2012, p. 249 - 252

Graphene-like microstructure of pyrolytic carbon from ethanol

S. ZHAO[*], JL. SHI, XH. WEI, X. YAN, QG. GUO, L. LIU
Key Laboratory of Carbon Materials, Institute of Coal Chemistry, Chinese academy of Sciences, Taiyuan 030001, China

Pyrolytic carbon (PC) from ethanol was deposited on the carbon monofilaments by cold-wall chemical vapour deposition. Scanning electron microscopy (SEM) and Raman spectroscopy were employed to characterize the features of PC. An interesting appearance of Raman spectra was obtained for the PC deposition at 1000 ℃. The value of I_{2700}/I_G is about 2.23 and the feature is similar to that of the chemical vapour deposited graphene. It was concluded that the feature was induced by the regular microstructure of crystal grains with few defect in the sp^2 domains.

(Received December 7, 2011; accepted February 20, 2012)

Keywords: Pyrolytic carbon, Ethanol, Coating, Microstructure

1. Introduction

Because of the high purity and controllable microstructure, pyrolytic carbon (PC) has attracted great interest in different research fields [1-4]. The carbon source used is mainly selected in a wide variety of hydrocarbon such as methane, propane and acetylene [5, 6]. As the precursor is one of the most important factors determining the microstructure of PC [7], an exploration of new precursors would promote the development of carbon relative materials.

Recently, ethanol has fascinated many researchers in the field of fabricating single wall carbon nanotubes with high purity at low temperature [8-12]. Compared with the traditional precursors, ethanol can avoid the co-exist appearance of amorphous carbon to a large extent during the pyrolysis process, which should be due to the existence of hydroxyl [13]. It has also been indicated that ethanol is a promising precursor for fabricating PC with unique microstructure [14]. However, the studies in this field were mainly focused on the hot-wall CVD. In this work, PC from ethanol was deposited on the carbon monofilament by cold-wall CVD and the microstructure was investigated.

2. Experimental

The laboratory-scale electrically heated cold-wall CVD reactor has been described by O. Féron et al. [15, 16]. Ethanol was used as carbon source and its vapour saturation was obtained with H_2 carrier gas going through a bubbler maintained at 30 ℃ (Pethanol=15.7 kPa). The ethanol concentration was subsequently adjusted by diluting the saturated ethanol/H_2 mixture in a further H_2 flow. For all the experiments, the total pressure and gas flows of H_2 (carrier) and H_2 (dilution) through the reactor were 101 kPa, 500 and 1500 cm^3/min respectively. A four-way valve was installed at the inlet of the reactor allowing the heating of the substrate under H_2/Ar atmosphere before the introduction of the reactive (ethanol/H_2) mixture.

The PC coatings were carried out in a cold-wall reactor consisting of a vertical glass tube (L=450 mm, φ=20 mm) connected to gas inlet/outlet flanges on both ends (respectively, on top/bottom). A fixed pitch based carbon monofilament was used as substrate. It was electrically heated with constant intensity supply. Three samples A, B, C were fabricated at 1000, 1100 and 1200 ℃, respectively.

The surface temperature was measured with a high-resolution bichromatic pyrometer (Ircon Mirage). The morphology of the coatings was characterized with a field emission gun scanning electron microscope (SEM) (Hitachi S-4800). Raman spectroscopy is a suitable method for determining the microstructure of carbon materials [14-19]. In this work, Raman microprobe (RMS) analyses (HP800 from JY, France) were conducted on the longitude surface of PC coated carbon fibers. The excitation source was a He-Ne laser (λ=532.8 nm). The resolution of the laser probe was close to 1μm and the depth analyzed was of the order of 100 nm.

3. Results

Fig. 1 show the SEM images of transverse and longitude surfaces of PC coatings deposited at different temperatures. It can be seen in Fig. 1A that for the PC coating deposited at 1000 ℃, the carbon monofilament is surrounded by a thick layer of PC with a rough hackly fracture surface, about 1μm in thickness, corresponding to the medium-textured PC. The SEM image at large magnification (Fig. 2A) shows that the inside surface of PC coating was relatively dense with fine striations running parallel to the carbon monofilament axis. These striations may be normally related to the inheritance of the longitude surface of pitch based carbon monofilament. As shown in Fig. 1B and 1C, multiple graphitic carbon layers arrange concentrically around the carbon monofilament. The parallel layer type structure indicates that PC seems to grow in the same lamellar way at high temperature. The SEM images of the PC layers deposited at 1100-1200 ℃ show growth character and preferred orientation, obviously corresponding to the high-textured carbon.

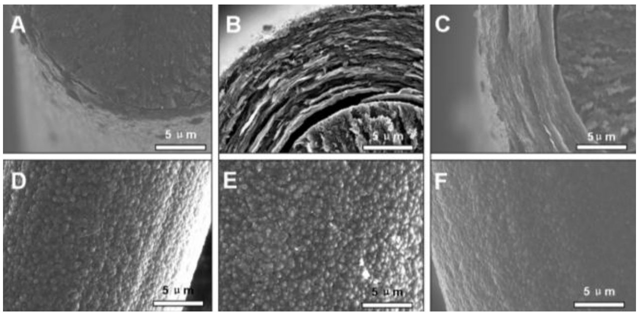

Fig. 1. SEM micrographs of PC coatings deposited at various temperatures: image A, B, and C correspond to the cross section of coatings deposited at 1000, 1100, and 1200 ℃, respectively; image D, E, and F correspond to the surface of PC coatings deposited at 1000, 1100, and 1200 ℃, respectively.

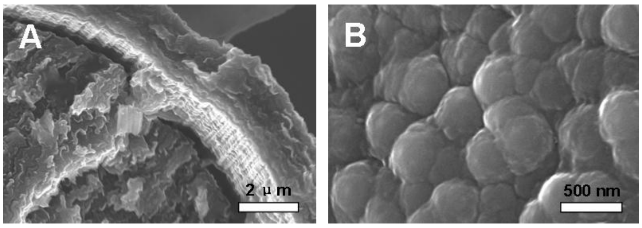

Fig. 2. SEM images with high resolution of cross-section (A) and longitude surface (B) of PC coatings deposited at 1000 ℃

In Fig. 1, it can be seen that the PC coatings display a longitude surface structure dominated by the presence of globular features. The number of these globular structures, their roughness and their sizes seem to decrease as deposition temperature is raised. The globular features obtained at 1000 ℃ present uniform and compact globules, with diameter of about 250 nm (Fig. 2B).

The spectra of Raman of PC coatings deposited at 1000, 1100, 1200 ℃ are displayed in Fig. 3, respectively. The Raman spectra of samples show a typical polycrystalline graphite structure with the D band (for disorder) at 1350 cm^{-1} and the G band (for graphite) at 1584 cm^{-1} [20]. The intensity ratio I_D/I_G and the full widths at half maximum (FWHM) of the D and the G band have been widely used to characterize the degree of in-plane crystallinity and the crystallite size of primary graphitic domains in carbons [21-26]. The intensity ratio I_D/I_G is inversely proportional to the crystallite size while the FWHM reflects the content of amorphous carbon. In addition, the appearance and shape of the second order 2D Raman spectrum with peak at about 2700 cm^{-1} can provide evaluation for the orientation of the crystallites in the three dimensional microstructure [27, 28].

According to Fig. 3, it can be seen that with the rise of deposition temperature, the D and second-order bands grow in intensity, whereas the FWHM of the G band decrease. These changes suggest that the in-plane disorder as well as the level of graphitization increases with the rise of temperature. It is notable that a single, sharp 2D peak in PC coating is measured in Fig. 3A and the intensity of 2D band is about 2 times higher than that of G band. This feature is much different from the Raman spectra of other samples. Notably, the G peak intensity in the Raman spectra of the three samples is comparable.

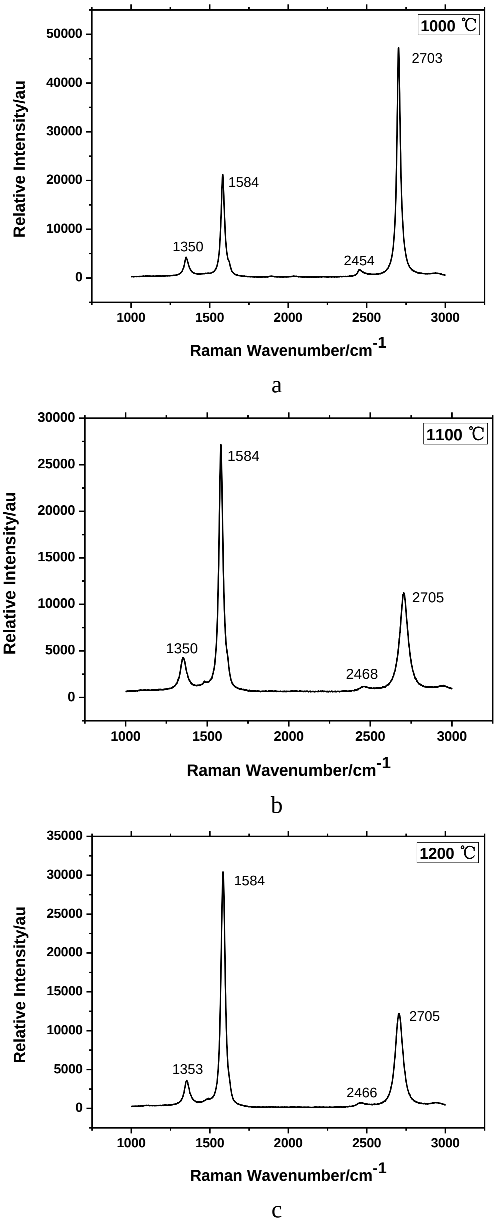

a

b

c

Fig. 3. Raman spectra of PC coatings deposited at 1000, 1100, and 1200 ℃, respectively.

Raman parameters for the PC coatings are shown in Table 1. The La value of crystal grain is also estimated by the value of R (I_D/I_G) according to the scale of the Tuinstra and Koenig relationship [20]. It can be seen that as deposition temperature increases, the value R and La decrease accordingly. The value of I_{2700}/I_G of sample A is about 2.23, which is much larger than that of the other two samples. It can be concluded that the PC coating deposited at 1000 ℃ has a distinctive microstructure which is much different from the other two samples investigated.

Table 1. Raman parameters for the PC coatings deposited at different temperature.

Sample	T (℃)	I_D/I_G	L_a (nm)	I_{2700}/I_G	$FWHM_D$ (cm^{-1})	$FWHM_G$ (cm^{-1})	$FWHM_{2700}$ (cm^{-1})
A	1000	0.18	24.44	2.23	35.1	26.9	27.3
B	1100	0.13	33.85	0.41	47.0	29.0	58.1
C	1200	0.10	44.00	0.40	41.7	28.7	53.7

4. Discussion

It has reported that the 2D peak in graphite consists of two peaks $2D_1$ and $2D_2$ while the 2D peak in on single grapheme layer has only one component with roughly four times the intensity of the G peak [29]. The higher intensity of the 2D peak relative to the G band in a graphene monolayer is due to the triple resonance activation mechanism [30]. Escribano et al. [31] have indicated that the very narrow and strong 2D band appeared in the Raman spectra of glass carbon can be attributed to a very regular structure. In our work, the 2D band of sample deposited at 1000℃ is also narrow and strong, indeed it is two times high than that of the G band. Only the graphene fabricated by CVD has a higher ratio of I_{2D}/I_G [32]. The graphene nanosheets produced by a soft chemistry synthesis route have a broad and weak 2D band and it was attributed to the significant decrease of the size of the in-plane sp^2 domains due to oxidation and ultrasonic exfoliation in the fabrication [33]. Thus, it can be concluded that though PC from ethanol deposited at 1000 ℃ has smaller crystal size than that of PC deposited at higher temperature, it has a regular structure with few defects in the sp^2 domains.

It is known that among the four dissociation reactions of ethanol as follows, the first two reactions are dominant under the current CVD conditions [34].

$$M + C_2H_5OH \rightarrow M + H_2O + C_2H_4 \quad (1)$$

$$M + C_2H_5OH \rightarrow M + CH_2OH + CH_3 \quad (2)$$

$$M + C_2H_5OH \rightarrow M + CH_3HCO + H_2 \quad (3)$$

$$M + C_2H_5OH \rightarrow M + OH + C_2H_5 \quad (4)$$

Park et al. [35] have studied the mechanism for thermal decomposition of ethanol using Ab initio molecular orbital theory. It is indicated that at lower temperature, the decomposition of CH_3CH_2OH occurs primarily by the dehydration reaction (1) while the production of CH_3+CH_2OH following reaction (2) becomes dominant when temperature is over 1200 ℃. In our work, it is assumed that the dehydration reaction which is dominant at low temperature may be the reason for the formation of PC coating with the unique microstructure. The appearance of H_2O may suppress the generation of amorphous carbon and promotes the formation of crystal grains with regular microstructure.

5. Conclusion

The microstructure of PC coating from ethanol is greatly determined by the deposition temperature in cold-wall CVD. The PC coating obtained at 1000 ℃ has a regular microstructure with few defects in the sp^2 domains. The microstructure of PC coating from ethanol is closely related to the change of dominant species in the gas phase at different temperature. H_2O which is dominant in the gas phase at low deposition temperature was presumed for the cause of the formation of unique microstructure observed.

References

[1] S. Jasieńko, J. Machnikowski, Carbon. **19**, 199 (1981).
[2] Y. X. Zhao, C. W. Bowers, I. L. Spain, Carbon. **26**, 291 (1988).
[3] D. B. Murphy, R. W. Carroll, Carbon. **30**, 47 (1992).
[4] V. D. Pauw, J. Hawecker, R. Schneider, W. Send, X. L. Wang, D. Gerthsen, Carbon, **46**, 236 (2008).
[5] A. Becker, K. J. Hüttinger, Carbon, **36**, 177 (1998).
[6] A. Becker, K. J. Hüttinger, Carbon, **36**, 201 (1998).
[7] W. Benzinger, A. Becker, K. J. Hüttinger, Carbon, **34**, 957 (1996).
[8] S. Chiashi, Y. Murakami, Y. Miyauchi, S. Maruyama, Chem. Phys. Lett, **386**, 89 (2004).
[9] Y. L. Li, L. A. Kinloch, A. H. Windle, Science, **304**, 276 (2004).
[10] L. M. Huang, X. D. Cui, B. White, S. P. O'Brien, J. Phys. Chem. B, **108**, 16451 (2004).
[11] A. Grüneis, M. H. Rümmeli, C. Kramberger, A. Barreiro, T. Pichler, R. Pfeiffer, H. Kuzmany, T. Gemming, B. Büchner, Carbon, **44**, 3177 (2006).

[12] R. Xiang, E. Einarsson, J. Okawa, Y. Miyauch, S. Maruyama, J. Phys. Chem. C, **113**, 7511 (2009).
[13] S. Maruyama, Y. Miyauchi, Y. Murakami, S. Chiashi, New. J. Phys, **5**, 149 (2003).
[14] A. J. Li, S. Y. Zhang, B. Reznik, S. Lichtenberg, O. Deutschmann, Ind. Eng. Chem. Res, **49**, 10421 (2010).
[15] O. Féron, G. Chollon, F. Dartigues, F. Langlais, R. Naslain, Diamond. Relat. Mater, **11**, 1234 (2002).
[16] R. V. Krishnarao, J. Subrahmanyam, S. Subbarao, Bull. Mater, **24**, 273 (2001).
[17] T. Jawhari, A. Roid, J. Casado, Carbon, **33**, 1561 (1995).
[18] M. Benlahsen, M. Therasse, Carbon, **42**, 2255 (2004).
[19] A. Sadezky, H. Muckenhuber, H. Grothe, R. Niessner, U. Pöschl, Carbon, **43**, 1731 (2005).
[20] F. Tuinstra, J. L. Koenig, J. Chem. Phys, **53**, 1126 (1970).
[21] Y. L. Huang, R. J. Young, J. Mater. Sci, **29**, 4027 (1994).
[22] P. Lespade, R. Al-Jishi, M. S. Dresselhaus, Carbon, **20**, 427 (1982).
[23] S. L. Lu, C. Blanco, B. Rand, Carbon, **40**, 2109 (2002).
[24] T. W. Scharf, I. L. Singer, Thin Solid Films, **440**, 138 (2003).
[25] G. A. Zickler, B. Smarsly, N. Gierlinger, H. Peterlik, O. Paris, Carbon, **44**, 3239 (2006).
[26] M. Mann, G. E. Shter, G. S. Grader, J. Mater. Sci, **41**, 6046 (2006).
[27] R. J. Nemanich, S. A. Solin, Phys. Rev. B, **20**, 392 (1979).
[28] G. Hackl, H. Gerhard, N. Popovska, Thin Solid Films, **513**, 217 (2006).
[29] N. Ferralis, J. Mater. Sci, **45**, 5325 (2010).
[30] M. Malard, M. Pimenta, G. Dresselhaus, M. Dresselhaus, Phys. Rep, **473**, 51 (2009).
[31] R. Escribano, J. J. Sloan, N. Siddique, N. Sze, T. Dudev, Vib. Spectrosc, **26**, 179 (2001).
[32] A. C. Ferrari, J. C. Meyer, V. Scardaci, C. Casiraghi, M. Lazzeri, F. Mauri, S. Piscanec, D. Jiang, K. S. Novoselov, S. Roth, A. K. Geim, Phys. Rev. Lett, **97**, 187401 (2006).
[33] G. X. Wang, J. Yang, J. Park, X. L. Gou, B. Wang, H. Liu, J. Yao, J. Phys. Chem. C, **112**, 8192 (2008).
[34] A. Li, S. Zhang, B. Reznik, S. Lichtenberg, G. Schoch, O. Deutschmann, Proceeding of the Combustion Institute, **33**, 1843 (2011).
[35] J. Park, R. S. Zhu, M. C. Lin, J. Chem. Phys, **117**, 3224 (2002).

---

[*] Corresponding author: zsbird1223@yahoo.com.cn